
Constrained Parameter Inference as a Principle for Learning

Nasir Ahmad Ellen Schrader Marcel van Gerven

Department of Artificial Intelligence

Donders Institute for Brain, Cognition and Behaviour

Radboud University, Nijmegen, the Netherlands

{n.ahmad,e.schrader,m.vangerven}@donders.ru.nl

Abstract

Learning in biological and artificial neural networks is often framed as a problem in which targeted error signals are used to directly guide parameter updating for more optimal network behaviour. Backpropagation of error (BP) is an example of such an approach and has proven to be a highly successful application of stochastic gradient descent to deep neural networks. However, BP relies on the transmission of gradient information directly to parameters, and frames learning as two completely separated passes. We propose constrained parameter inference (COPI) as a new principle for learning. The COPI approach to learning proposes that parameters might infer their updates based upon local neuron activities. This estimation of network parameters is possible under the constraints of decorrelated neural inputs and top-down perturbations of neural states, where credit is assigned to units instead of parameters directly. The form of the top-down perturbation determines which credit assignment method is being used, and when aligned with BP it constitutes a mixture of the forward and backward passes. We show that COPI is not only more biologically plausible but also provides distinct advantages for fast learning when compared to BP.

1 Introduction

Learning can be defined as the ability of natural and artificial systems to adapt to changing circumstances based on their experience. In biological and artificial neural networks this requires updating of the parameters that govern the network dynamics [33].

A principled way of implementing learning in artificial neural networks is through the backpropagation of error (BP) algorithm [1, 7]. BP is a gradient-based method which uses reverse-mode automatic differentiation to compute the gradients that are needed for individual parameter updating [27]. This approach relies on the repeated application of forward and backward passes through the network. In the forward (inference) pass, network activity is propagated forward to compute network outputs. In the backward (learning) pass, the loss gradient associated with the network outputs is propagated in the reverse direction for parameter updating.

While effective, BP makes use of the transmission of gradients using biologically implausible non-local operations, and multiple separated network passes [3, 4, 37]. Alternative approaches, such as Hebbian learning and subspace methods circumvent this problem yet are restricted to unsupervised learning and do not afford (deep) credit assignment [17, 20].

Here, we propose constrained parameter inference (COPI) as a new principle for learning. COPI uses information that can be made locally available at the parameter being inferred under certain constraints. Note that COPI is distinct from methods that rely on measuring gradients through activity

differences (see the NGRAD hypothesis [37]), in that no difference in activity needs to be computed to determine parameter updates. Specifically, with a single mixed network activity state – in the BP case a mixture of the forward and backward pass – the parameters can infer their new values. This is distinct to the many biologically plausible methods which require parameters to measure differences in some activity, either physically using separate compartments/signals, or across time between two phases [14, 25, 26, 29, 36, 40]. Thus COPI is a stepping stone toward online continuous learning where parameter updates are based upon single state measurements.

Furthermore, the COPI algorithm is not tied to any particular credit assignment method. Instead it simply assumes that unit activities might be shifted by top-down perturbations. The form of the perturbation is precisely what determines which credit-assignment algorithm is being used for learning within the system, whether based on backpropagation, feedback alignment [22, 23], target propagation [14, 35] or otherwise.

In the following, we demonstrate that COPI provides a powerful framework for learning which is at least as effective as backpropagation of error while having the potential to rely on local operations only. This has direct implications for modern machine learning as COPI can be used as a plug-in replacement of backpropagation in a range of settings.

2 Methods

In this section, we develop the constrained parameter inference (COPI) approach and describe its use for parameter estimation in feedforward neural networks.

2.1 Deep neural networks

Let us consider deep neural networks consisting of L layers. The input-output transformation in layer l is given by

$$y_l = f(a_l) = f(W_l x_l)$$

with output y_l , activation function f , activation $a_l = W_l x_l$, input x_l and weight matrix $W_l \in \mathbb{R}^{K_l \times K_{l-1}}$, where K_l indicates the number of units in layer l . As usual, the input to a layer $l > 1$ is given by the output of the previous layer, that is, $x_l = y_{l-1}$. Learning in deep neural networks amounts to determining for each layer in the network a weight update Δ_{W_l} such that the update rule

$$W_l \leftarrow W_l + \eta \Delta_{W_l}$$

converges towards those weights that minimize a loss ℓ for some dataset \mathcal{D} for some suitable learning rate $\eta > 0$. Locally, the optimum by gradient descent (GD) is to take a step in the direction of the negative expected gradient of the loss. That is,

$$\Delta_{W_l}^{\text{gd}} = -\mathbb{E}[\nabla_{W_l} \ell],$$

where, in practice, the expectation is taken under the empirical distribution.

2.2 Constrained parameter inference in feedforward systems

Here, we develop an alternative approach and relate it directly to both stochastic gradient descent and local parameter inference. The key transformation in a deep feedforward neural network is carried out by a weight matrix given by

$$a_l = W_l x_l.$$

Suppose we know the desired target state z_l for this transformation. This can be expressed as an alternative transformation

$$z_l = D_l x_l$$

for some desired weight matrix D_l . Ideally, we would use a learning algorithm which could guarantee a convergence of the current weight matrix. A straightforward proposal is to carry out a decay from the current weight values to the desired weight values, such that the weight update is of the form

$$\Delta_{W_l} = \mathbb{E}[D_l - W_l] = D_l - W_l. \quad (1)$$

The key goal is to achieve this weight update without making use of the (unknown) desired weight matrix.

2.3 Learning the forward weights

Let us rewrite the desired weight matrix in the following way:

$$\begin{aligned} D_l &= D_l \left(\mathbb{E} [x_l x_l^\top] \mathbb{E} [x_l x_l^\top]^{-1} \right) \\ &= \mathbb{E} [D_l x_l x_l^\top] \mathbb{E} [x_l x_l^\top]^{-1} \\ &= \mathbb{E} [z_l x_l^\top] \mathbb{E} [x_l x_l^\top]^{-1} \end{aligned}$$

with $\mathbb{E} [x_l x_l^\top]$ the expected (empirical) correlation matrix, which we assume to be invertible, though this condition is later shown to be unnecessary. If we plug this back into Eq. (1) then we obtain

$$\Delta_{W_l} = \mathbb{E} [z_l x_l^\top] \mathbb{E} [x_l x_l^\top]^{-1} - W_l, \quad (2)$$

allowing the weight update to be expressed in terms of target outputs, z_l , rather than (unknown) desired weights.

Let us assume for the moment that the inputs x_l are distributed such that they have zero covariance and unit variance, i.e., the inputs are whitened. This implies that the expected correlation matrix is given by the identity matrix, that is, $\mathbb{E} [x_l x_l^\top] = I$. In this case, Eq. (2) reduces to the simple update rule

$$\Delta_{W_l} = \mathbb{E} [z_l x_l^\top] - W_l.$$

In practice, it may be unreasonable (and perhaps even undesirable) to assume perfectly whitened input data. A more realistic and achievable scenario is one in which we make the less restrictive assumption that the data is decorrelated rather than whitened. This implies that the expected correlation matrix is diagonal, that is, $\mathbb{E} [x_l x_l^\top] = \text{diag} (\mathbb{E} [x_l^2])$. Here, $x_l^2 = x_l \circ x_l$ is the vector of squared elements of x with \circ the Hadamard product. Right-multiplying both sides of Eq. (2) by this expression, and assuming that $\mathbb{E} [x_l x_l^\top]$ is indeed diagonal, we obtain

$$\Delta_{W_l} \text{diag} (\mathbb{E} [x_l^2]) = \mathbb{E} [z_l x_l^\top] - W_l \text{diag} (\mathbb{E} [x_l^2]).$$

This amounts to a rescaling of the rows of Δ_{W_l} , akin to a scaling of the learning rate of the rows of this matrix. This finally leads to our constrained parameter inference (COPI) learning rule

$$\Delta_{W_l}^{\text{copi}} = \mathbb{E} [z_l x_l^\top] - W_l \text{diag} (\mathbb{E} [x_l^2]), \quad (3)$$

which is solely composed of a correlational, Hebbian, learning term and a weight decay term. COPI receives its name from the fact that there are two constraints in play. First, the availability of a target or ‘desirable’ state z_l for each layer and, second, the requirement that the inputs x_l are decorrelated.

2.4 Input decorrelation

We did not yet address how to ensure that the inputs to each layer are decorrelated. To this end, we introduce a new decorrelation method which transforms the potentially correlation-rich outputs y_{l-1} of a layer into decorrelated inputs x_l to the following layer using the transformation

$$x_l = R_l y_{l-1},$$

where R_l is a decorrelating ‘lateral’ weight matrix.

Let us consider attempting to reduce the correlation in the output data, x_l , by measurement of its correlation and a shift toward lower correlation. In particular, consider a desired change in a given sample of the form

$$x_l \leftarrow x_l - \eta (\mathbb{E} [x_l x_l^\top] - \text{diag} (\mathbb{E} [x_l^2])) x_l,$$

where the expectations could be taken over the empirical distribution. We can shift this decorrelating transformation from the output activities x_l to the decorrelating matrix R_l . To do so, consider substituting $x_l = R_l y_{l-1}$, such that we may write

$$\begin{aligned} x_l &\leftarrow x_l - \eta (\mathbb{E} [x_l x_l^\top] - \text{diag} (\mathbb{E} [x_l^2])) x_l \\ &\leftarrow R_l y_{l-1} - \eta (\mathbb{E} [x_l x_l^\top] - \text{diag} (\mathbb{E} [x_l^2])) R_l y_{l-1} \\ &\leftarrow (R_l - \eta (\mathbb{E} [x_l x_l^\top] - \text{diag} (\mathbb{E} [x_l^2]))) R_l y_{l-1}. \end{aligned}$$

We converge to the optimal decorrelating matrix R_l^* using an update $R_l \leftarrow R_l + \eta \Delta_{R_l}^{\text{copi}}$ with

$$\Delta_{R_l}^{\text{copi}} = -(\mathbb{E}[x_l x_l^\top] - \text{diag}(\mathbb{E}[x_l^2])) R_l.$$

Assuming that R_l is initialised symmetrically, for example with the identity matrix, this matrix update maintains the symmetry of R_l and hence we may equivalently write this as

$$\begin{aligned} \Delta_{R_l}^{\text{copi}} &= -(\mathbb{E}[x_l x_l^\top] R_l - \text{diag}(\mathbb{E}[x_l^2]) R_l) \\ &= -(\mathbb{E}[q_l x_l^\top] - R_l \text{diag}(\mathbb{E}[x_l^2])) \end{aligned} \quad (4)$$

with $q_l = R_l x_l$. This has exactly the same form as our previous COPI rule for learning the forward weights though now acting via lateral weights to ‘inhibit’ (note the negative sign in the weight update) correlations, again using target states q_l . Hence, we are invoking the same principle to learn both the forward and lateral weights! Note that in reality these lateral weights are not strictly ‘inhibitory’ in the neuroscientific sense, but act to reduce correlation by providing either positive or negative feedback. In effect, the lateral weights are also constantly inferring correlational structure within the activities of a layer of units but, given the negatively-signed update, they update their values to reduce correlation.

2.5 Error signals

Equation (3) expresses learning of forward weights in terms of target states z_l . However, without access to targets for each layer of a deep neural network model, one may ask how this learning approach could be applied. To this end, we assume that the target states can be expressed as

$$z_l = a_l + \delta_l$$

with δ_l an error signal which perturbs the neuron’s state in a desired direction. According to stochastic gradient descent (SGD), the optimal perturbation is given by

$$\delta_l^{\text{sgd}} = -\frac{d\ell}{da_l}$$

as this guarantees that the neuronal states are driven in the direction of locally-decreasing loss. The error signal at the output layer is given by

$$\delta_L \triangleq \delta_L^{\text{sgd}} = -\frac{\partial \ell}{\partial a_L} = -\text{diag}(f'(a_L)) \frac{\partial \ell}{\partial y_L}.$$

Starting from $\delta_L^{\text{bp}} = \delta_L$, the SGD perturbation can be computed via backpropagation (BP) by propagating the error signal from output to input according to

$$\delta_l^{\text{bp}} = \frac{\partial a_{l+1}}{\partial a_l} \delta_{l+1}^{\text{bp}}$$

with

$$\begin{aligned} \frac{\partial a_{l+1}}{\partial a_l} &= \frac{\partial y_l}{\partial a_l} \frac{\partial x_{l+1}}{\partial y_l} \frac{\partial a_{l+1}}{\partial x_{l+1}} \\ &= \frac{\partial f(a_l)}{\partial a_l} \frac{\partial R_{l+1} y_l}{\partial y_l} \frac{\partial W_{l+1} x_{l+1}}{\partial x_{l+1}} \\ &= \text{diag}(f'(a_l)) R_{l+1}^\top W_{l+1}^\top. \end{aligned}$$

While this provides a gold standard for the optimal perturbation, ideally, we would like to replace this by more biologically-plausible credit assignment methods that do not make use of gradient information. We explore alternatives below, though each of these methods uses the same error signal δ_L for the output layer but propagates the error signal in the input direction using different proposal mechanisms.

Feedback alignment

Feedback alignment (FA) supposes that the perturbation from the previous layer can be propagated through fixed random top-down weights B_{l+1} instead of the transposed weight matrix $(W_{l+1} R_{l+1})^\top$ [22]. Hence, the layer-wise perturbations are propagated by

$$\delta_l^{\text{fa}} = \text{diag}(f'(a_l)) B_{l+1} \delta_{l+1}^{\text{fa}}.$$

Potential for alternative credit-assignment methods

In this work, we specifically compare backpropagation and feedback alignment. However, alternative methods of credit assignment could also be arbitrarily integrated within the COPI approach.

For example, direct feedback alignment makes use of a random projection of the output node errors to the rest of the network [23]. That is, we could construct layer-wise perturbations where

$$\delta_l^{\text{dfa}} = \text{diag}(f'(a_l))B_{l+1}\delta_L^{\text{dfa}}.$$

An example of a different flavour of credit assignment would be target propagation, which supposes that credit is assigned by a top-down, autoencoder-esque, pass from the target output toward the input [14]. Supposing a top-down (approximate) inverse model, using weight matrices B_{l+1} , exists for every layer l , where $f(B_{l+1}y_{l+1}) \approx y_l$, this can be integrated with COPI using a perturbation

$$\delta_l^{\text{tp}} = f(B_{l+1}\delta_{l+1}^{\text{tp}}) - a_l,$$

which indicates a perturbation away from the current activation, a_l , and toward the inverse model $f(B_{l+1}\delta_{l+1}^{\text{tp}})$ of the perturbation from the layer above. Target propagation is not directly related to backpropagation but a more direct theoretical relationship could also be established via methods such as GAIT propagation [35].

2.6 Stochastic COPI

Stochastic COPI replaces the expectations over the empirical distributions in Eqs. (3) and (4) by single data points, as in stochastic gradient descent (SGD). COPI training on single data points proceeds by computing the stochastic weight updates

$$\Delta_{W_l}^{\text{copi}} = z_l x_l^\top - W_l \text{diag}(x_l^2) \quad (5)$$

$$\Delta_{R_l}^{\text{copi}} = -(q_l x_l^\top - R_l \text{diag}(x_l^2)) \quad (6)$$

with target states $z_l = a_l + \delta_l$ and $q_l = R_l x_l$ given some suitable error signal δ_l . Figure 1 provides an overview of the computational operations that are in play. See the Appendix A for a pseudo-algorithm. In practice, we train on minibatches instead of individual data points.

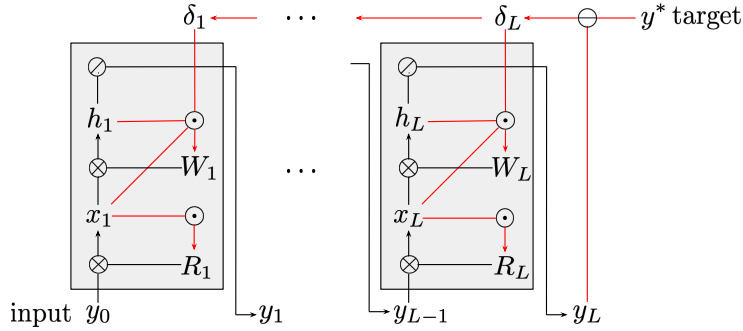


Figure 1: **COPI learning in a deep feedforward neural network.** Gray boxes represent COPI layers, with forward passes indicated in black and backward passes indicated in red. Parameter updates (5) and (6) indicated by \ominus . Matrix multiplication indicated by \otimes . Activation function application indicated by \odot . Loss computation indicated by \oplus . Self-dependencies not shown.

2.7 Correspondence to stochastic gradient descent

For comparison against SGD, it is instructive to consider (stochastic) COPI in the case of a single-layer neural network which is acting on decorrelated inputs. Recall that the SGD update of a single-layer network is given by

$$\Delta_W^{\text{sgd}} = -\frac{dl}{da} x^\top.$$

We can manipulate this expression in order to relate SGD to COPI as follows:

$$\begin{aligned}\Delta_W^{\text{sgd}} &= -\frac{d\ell}{da}x^\top \\ &= \left(a - \frac{d\ell}{da}\right)x^\top - ax^\top \\ &= (a + \delta^{\text{sgd}})x^\top - W(xx^\top).\end{aligned}$$

Comparing this final expression of the SGD update, to the (stochastic) COPI update, namely $\Delta_W^{\text{copi}} = (a + \delta)x^\top - W \text{diag}(x^2)$, clearly, in this special case, the SGD update and the COPI update with error signal δ^{sgd} are approximately equivalent. The key difference here is that COPI specifically assumes that there are decorrelated inputs and therefore the weight decay term is unaffected by sample-wise input cross-correlations, whereas SGD’s weight decay is modified by sample-wise input cross-correlations which could eventually average out to a diagonal matrix in the case of decorrelated inputs.

2.8 Code, implementation, and compute

Code, pseudocode, computational implementation details, and additional mathematical explanations of the methods used to produce all plots in the results which follow are provided in the Appendices.

3 Results

In the following, we analyse both the convergence properties of COPI and the benefits of the decorrelated representations at every network layer.

3.1 COPI performance on standard benchmarks

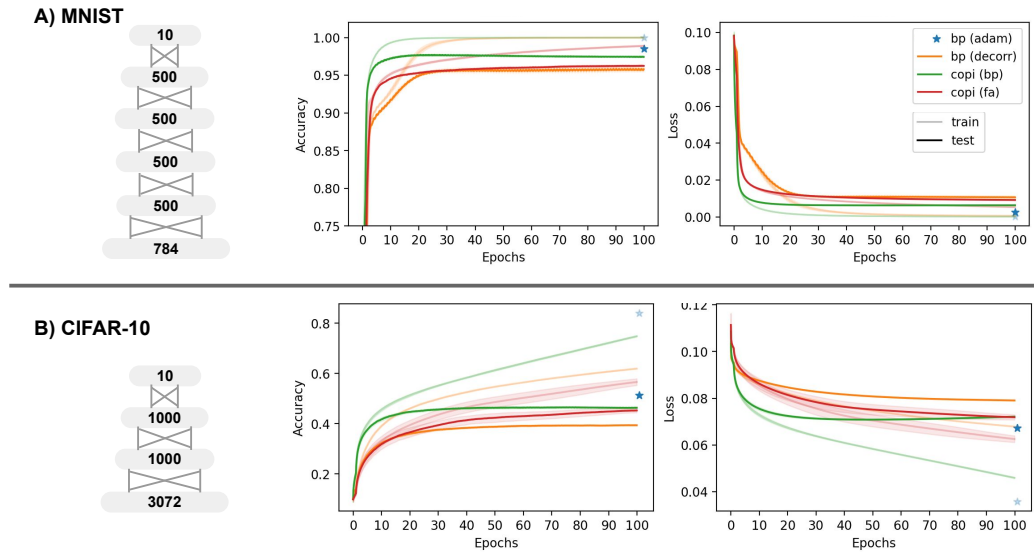


Figure 2: **COPI vs BP performance on standard computer vision classification tasks.** A) Train/test accuracy and loss of a five-layer (784-500-500-500-10, layer sizes), fully-connected, feedforward deep neural network model trained and tested on the handwritten MNIST dataset. B) Train/test accuracy of a three-layer (3072-1000-1000-10), fully-connected, feedforward deep neural network model trained and tested on the CIFAR-10 dataset. All networks were run with five random seeds and envelopes show standard deviation across these networks.

To validate COPI as a principle for learning, we compared it against backpropagation by training fully-connected deep feedforward neural networks trained on the MNIST handwritten digit dataset [42] (License: CC BY-SA 3.0) and the CIFAR-10 image dataset [10] (License: MIT).

COPI was simulated together with both BP-based (δ_l^{bp}) and FA-based (δ_l^{fa}) perturbations with a loss function composed of the quadratic loss between network outputs and the one-hot encoded labels as ‘desired’ output. To clarify the benefits of the COPI algorithms, we additionally trained networks in which the weights, W_l , were updated by BP, and lateral weights were introduced and trained by the COPI decorrelating algorithm (Eq. 6). A baseline with backpropagation alone was also computed, where a network with no layer-wise decorrelating transformations was optimized to peak accuracy with the Adam optimizer [15].

Networks were constructed with the leaky rectified linear unit (leaky-ReLU) activation function. Otherwise the network transformations are described in the methods above and via pseudocode in Appendix A. Training was carried out in mini-batches of size 50 for all simulations (stochastic updates computed within these mini-batches are averaged during application). For the simulations involving the MNIST handwritten digit dataset, the learning rate of the simulations began at 10^{-2} for the first epoch, to ensure that the decorrelation could set in, and was thereafter boosted to 10^{-1} . This was carried out for all simulations aside from Adam (constant parameters: learning rate = 10^{-4} , $\beta_1 = 0.9$, $\beta_2 = 0.99$). For CIFAR-10, learning rates underwent the same change but began at 10^{-3} and were increased to 10^{-2} after the first epoch. Again, the Adam trained BP network was not subject to these learning rates (see above parameters). This learning rate adjustment after the first epoch was useful as unit activities are significantly reduced by the decorrelating procedure and this results in a lower effective learning rate and slower convergence. Thus, after an initial epoch of training which stabilised the decorrelation, we boosted the learning rates for all simulations which make use of decorrelation. Learning rates for the forward and lateral weight matrices were kept the same at all times.

Figure 2 shows the results of these simulations. Notably, during training, COPI is more successful as a learning rule compared to BP in the presence of decorrelation, despite having equivalent learning rates and very similar learning rules. We attribute this benefit to the explicit knowledge, built into the COPI learning rule, that inputs shall reach a decorrelated state. By comparison, BP updates are computed without this explicit knowledge and are therefore negatively affected by sample/mini-batch correlations, see Section 2.7.

Not only in terms of accuracy, but also in terms of speed, COPI shows rapidly convergence. It is important to note that BP with momentum does converge faster in general and reaches peak performance quickly. However, given that no other simulations made use of momentum (a stable approach for this is unclear in the face of decorrelation), we do not show or compare the convergence speed in the case of momentum. Furthermore, test performance of COPI is on par with BP, though multiple methods begin to show signs of overfitting in this network setup. Third, competitive performance is even obtainable using feedback alignment, with a continuing benefit of the use of the COPI algorithm. This suggests that attempts to make the BP signal more biologically plausible and local might prove more successful with COPI.

3.2 Decorrelation for feature analysis and network compression

The COPI algorithm’s requirement for decorrelation at every network layer is not only a restriction but also proves beneficial in a number of ways. We explore the decorrelation, as well as the analyses and computations that it enables.

The proposed decorrelation method produces a representation similar to existing whitening methods, such as ZCA [6]. Figure 3A provides a visualisation of a randomly selected set of data samples from the MNIST dataset. From top to bottom are shown: the unprocessed samples, samples processed by the first decorrelating layer of a network trained on MNIST with the COPI algorithm (see MNIST networks described in Figure 2), and finally a visualisation of samples transformed by a ZCA transform computed on the whole training set. As can be seen, there is qualitative similarity between the COPI- and ZCA-processed data samples. Remaining differences are attributed to the fact that COPI does not scale the individual elements of these samples (pixels) for unit variance, i.e. whitening, but instead produces decorrelation.

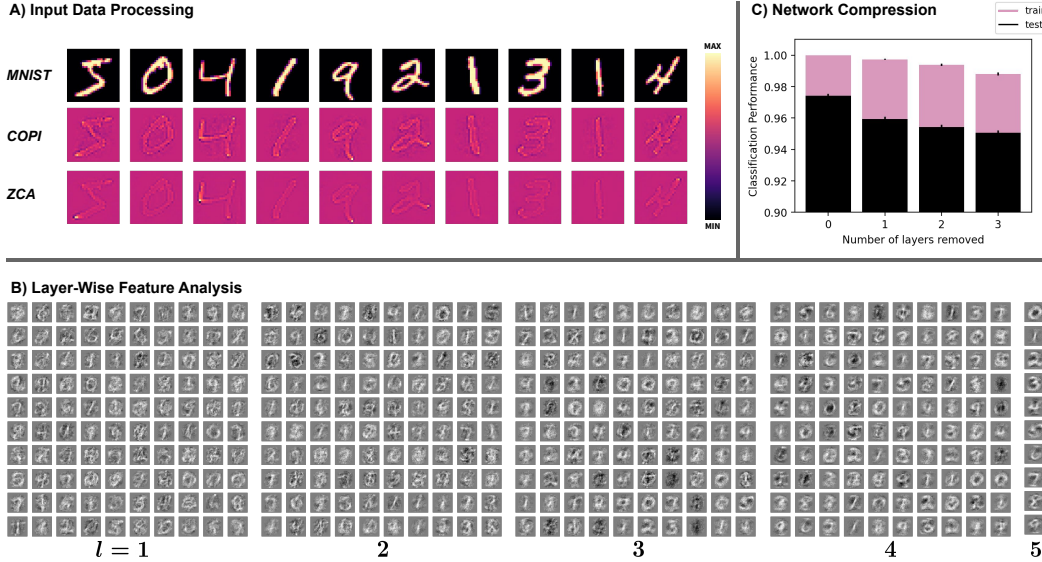


Figure 3: **The effect of whitening of the input layer activities, and decoded features across layers of a COPI network.** A) Visualisation of the MNIST dataset (top), the decorrelating transformation produced by the COPI algorithm (middle), and, the whitening transformation produced by ZCA whitening (bottom). B) Using the decorrelated network inputs of the COPI networks (see middle row in A), the decorrelated inputs, x_0 , from the entire training set data could be (pixel-wise) correlated with the network’s layer-wise outputs, y_l (node-wise). This produced a linear approximation of the units’ preferred features. C) The decorrelated layer-wise inputs of COPI-trained networks could also be used to efficiently infer linear mappings between distant layers of the network. This allows the removal of layers of a network and replacement with an inferred, linear approximation of those intermediate layers. Plotted are the performances of the 5-layer MNIST-trained COPI networks of Figure 2 with up to 3 hidden layers replaced with a single weight matrix. This process is repeated for five, randomly seeded networks and error bars show standard deviation across these repeats.

Beyond the input transformation, our COPI setup allows some interesting analyses, courtesy of the decorrelated layer-wise inputs. For visualisation of receptive fields of units deep within the network, we can make use of the decorrelated input training dataset (visualised Figure 3A) in order to form a linear approximation of the receptive field of units deep in the network. For each decorrelated input unit, that is, each element of x_0 , we can correlate its activity across the entire training set with the corresponding activity of any unit in the network. This provides an average, linear, feature response for each unit of y_l in a given layer. Figure 3B shows such extracted features from a random selection of 100 units from each layer of a COPI-trained network (ten for the final layer, which only holds 10 units). This allows us to observe an increasingly digit-oriented feature preference for units in our COPI-trained network, as we go deeper into the network, and the presence of digit selective and ‘anti-digit’ selective units.

This same mechanism of producing a linear approximation of RFs, also provides a computationally simple method to approximate the transformation produced by multiple layers of a COPI-trained network with a linear matrix. Appendix B provides an exploration on how this approximation can be made and why this is particularly efficient in these networks with decorrelated activities. We are therefore able to easily convert our MNIST trained network of five layers into networks of any smaller number of layers, effectively providing a straightforward approach for network compression. Figure 3C shows the performance impact of such conversions when five-layer MNIST-trained COPI networks have their hidden layers successively removed and instead approximated with a linear matrix. Note that this approximation is done in a single step using the network’s response to the training data and does not require any re-training. Given this, the network performance stays relatively high despite the approximation and removal of layers. The ability to achieve this network compression efficiently is a unique benefit of the decorrelated unit activities at every network layer.

4 Discussion

In this paper, we introduced constrained parameter inference (COPI) as a new approach to learning in feed-forward neural networks.

We derived an effective local learning rule and showed that, under the right conditions, individual weights could infer their own values. The locality required the removal of confounding influences between unit activities within every layer of the neural network. To this end, we derived an efficient decorrelation rule which, itself, is a special case of constrained parameter inference. We further assumed error signals were available to perturb unit activations towards more desirable states from which the system could learn.

A drawback of this current work was that we assumed that error signals were available and did not interfere with ongoing network activity. For a fully online and consistent implementation, the error machinery should be integrated into a single mixed pass. Resolving this tension is an area for future exploration. Beyond this, it is important to expand the datasets to which COPI has been applied and investigate its application to more exotic architectures.

Regardless, the resulting algorithm allowed us to effectively train deep feedforward neural networks, where performance is competitive with that of backpropagation for both gradient-based and feedback alignment signals. The algorithm also allows for more interpretable deep learning via the visualisation of deep decorrelated features [34] and contributes to efficient deep learning as it facilitates network compression [41].

COPI relates to unsupervised methods for subspace learning [2, 5, 17]. In particular, the form of the learning rule we propose bears a resemblance to Oja’s rule [2], see the Appendix C for a comparison, though it focuses on inference of parameters in the face of perturbations instead of latent factor extraction.

Aside from unsupervised methods, the inference of parameters based upon input and output activities has been previously proposed to overcome the weight-transport problem [30, 32, 39]. In particular, these methods attempt to learn the feedback connectivity required for backpropagation via random stimulation of units and a process of weight inference. Our method similarly attempts to carry out weight inference, but does so without random stimulation and with the purpose of learning of the forward model through combination with top-down perturbations.

It is also interesting to note that our decorrelating mechanism captures some of the key elements of batch normalization [16, 28]. First, vanilla batch-normalization makes use of demeaning, a natural outcome of our decorrelation. Furthermore, whitening of batches has been recently shown to be an extremely effective batch-wise processing stage, yielding state-of-the-art performance on a number of challenging classification tasks [28].

COPI may also shed light on learning and information processing in biological systems. There is both experimental and theoretical evidence that input decorrelation is a feature of neural processing through a number of mechanisms including inhibition, tuning curves, attention, and eye movements [6, 8, 9, 11, 12, 18, 19, 24, 31]. In particular, center-surround filters of the LGN appear to produce a form of whitening. Whitening also appears to be key for sparse coding of visual inputs [13]. To what extent there is decorrelation between all units projecting to a neuron is of course questionable, though COPI has the potential for modification to account for global or local correlations.

Beyond this, inhibitory and excitatory balance [21] has been formulated in a fashion which can be viewed as encouraging decorrelation. Learning rules which capture excitatory/inhibitory balance, such as the one by Vogels et al. [11], rely on correlative inhibition between units, which in turn reduce the inter-unit covariance. Such detailed balance has been observed across cortical areas and so it does not seem unreasonable to consider this as a method to encourage decorrelation of not just the input but also downstream ‘hidden’ layers of neural circuits.

Concluding, we argue that constrained parameter inference is not only a prime candidate to explore for biologically plausible learning but can also be treated as a plugin replacement of backpropagation for efficient and effective training of deep feedforward neural networks.

References

- [1] S. Linnainmaa. “The representation of the cumulative rounding error of an algorithm as a Taylor expansion of the local rounding errors”. In: *Master’s Thesis (in Finnish), Univ. Helsinki* (1970), pp. 6–7.
- [2] E. Oja. “Simplified neuron model as a principal component analyzer”. In: *Journal of Mathematical Biology* 15.3 (1982), pp. 267–273.
- [3] S. Grossberg. “Competitive learning: From interactive activation to adaptive resonance”. English. In: *Cognitive Science* 11.1 (1987), pp. 23–63.
- [4] F. Crick. “The recent excitement about neural networks”. In: *Nature* 337 (1989), pp. 129–132.
- [5] P. Földiák and M. P. Young. “Sparse coding in the primate cortex”. In: *The Handbook of Brain Theory and Neural Networks*. 1995.
- [6] A. J. Bell and T. J. Sejnowski. “The “independent components” of natural scenes are edge filters”. In: *Vision Research* 37.23 (1997), pp. 3327–3338.
- [7] P. J. Werbos. “Applications of advances in nonlinear sensitivity analysis”. In: *System Modeling and Optimization* (2005), pp. 762–770.
- [8] D. J. Graham, D. M. Chandler, and D. J. Field. “Can the theory of “whitening” explain the center-surround properties of retinal ganglion cell receptive fields?” In: *Vision Research* 46.18 (2006), pp. 2901–2913.
- [9] M. R. Cohen and J. H. R. Maunsell. “Attention improves performance primarily by reducing interneuronal correlations”. en. In: *Nature Neuroscience* 12.12 (Dec. 2009), pp. 1594–1600.
- [10] A. Krizhevsky. *Learning Multiple Layers of Features from Tiny Images*. Tech. rep. University of Toronto, 2009.
- [11] T. P. Vogels et al. “Inhibitory plasticity balances excitation and inhibition in sensory pathways and memory networks”. In: *Science* 334.6062 (2011), pp. 1569–1573.
- [12] X. Pitkow and M. Meister. “Decorrelation and efficient coding by retinal ganglion cells”. In: *Nature Neuroscience* 15.4 (2012), pp. 628–635.
- [13] P. D. King, J. Zylberberg, and M. R. DeWeese. “Inhibitory interneurons decorrelate excitatory cells to drive sparse code formation in a spiking model of V1”. en. In: *J. Neurosci.* 33.13 (Mar. 2013), pp. 5475–5485.
- [14] Y. Bengio. “How auto-encoders could provide credit assignment in deep networks via target propagation”. In: *ArXiv* (2014). ArXiv: 1407.7906 (cs.LG).
- [15] D. P. Kingma and J. Ba. “Adam: A method for stochastic optimization”. In: *ArXiv* (2014). ArXiv: 1412.6980 (cs.LG).
- [16] S. Ioffe and C. Szegedy. “Batch normalization: Accelerating deep network training by reducing internal covariate shift”. In: *ArXiv* (2015), pp. 1–11. ArXiv: 1502.03167 (cs.LG).
- [17] C. Pehlevan, T. Hu, and D. B. Chklovskii. “A Hebbian/anti-Hebbian neural network for linear subspace learning: A derivation from multidimensional scaling of streaming data”. In: *ArXiv* (2015). ArXiv: 1503.00669 (q-bio.NC).
- [18] I. Y. Segal et al. “Decorrelation of retinal response to natural scenes by fixational eye movements”. en. In: *Proceedings of the National Academy of Sciences U.S.A.* 112.10 (2015), pp. 3110–3115.
- [19] R. Abbasi-Asl et al. “Do retinal ganglion cells project natural scenes to their principal subspace and whiten them?” In: *2016 50th Asilomar Conference on Signals, Systems and Computers*. 2016, pp. 1641–1645.
- [20] J. Brea and W. Gerstner. “Does computational neuroscience need new synaptic learning paradigms?” In: *Current Opinion in Behavioral Sciences* 11 (2016), pp. 61–66.
- [21] S. Denève and C. K. Machens. “Efficient codes and balanced networks”. In: *Nature Neuroscience* 19.3 (2016), pp. 375–382.
- [22] T. P. Lillicrap et al. “Random synaptic feedback weights support error backpropagation for deep learning”. In: *Nature Communications* 7 (2016), p. 13276.
- [23] A. Nøkland. “Direct feedback alignment provides learning in deep neural networks”. In: *Advances in Neural Information Processing Systems* 29 (2016).
- [24] K. Franke et al. “Inhibition decorrelates visual feature representations in the inner retina”. en. In: *Nature* 542.7642 (2017), pp. 439–444.

- [25] B. Scellier and Y. Bengio. “Equilibrium Propagation: Bridging the Gap between Energy-Based Models and Backpropagation”. en. In: *Front. Comput. Neurosci.* 11 (May 2017), p. 24.
- [26] J. C. R. Whittington and R. Bogacz. “An approximation of the error backpropagation algorithm in a predictive coding network with local Hebbian synaptic plasticity”. In: *Neural Computation* 29.5 (May 2017), pp. 1229–1262.
- [27] A. G. Baydin et al. “Automatic differentiation in machine learning: a survey”. In: *Journal of Machine Learning Research* 18 (2018), pp. 1–43.
- [28] L. Huang et al. “Decorrelated batch normalization”. In: *Proceedings of the IEEE Computer Society Conference on Computer Vision and Pattern Recognition* (2018), pp. 791–800.
- [29] J. Sacramento et al. “Dendritic cortical microcircuits approximate the backpropagation algorithm”. In: *Advances in Neural Information Processing Systems 31*. Ed. by S. Bengio et al. Curran Associates, Inc., 2018, pp. 8721–8732.
- [30] M. Akrouf et al. “Deep learning without weight transport”. In: *ArXiv* (2019). ArXiv: 1904.05391 (cs.LG).
- [31] E. M. Dodds, J. A. Livezey, and M. R. DeWeese. “Spatial whitening in the retina may be necessary for V1 to learn a sparse representation of natural scenes”. In: *BioRxiv* (2019), pp. 1–15. DOI: doi:<https://doi.org/10.1101/776799>.
- [32] J. Guerguiev, K. P. Kording, and B. A. Richards. “Spike-based causal inference for weight alignment”. In: *ArXiv* (2019). ArXiv: 1910.01689 (q-bio.NC).
- [33] B. A. Richards et al. “A deep learning framework for neuroscience”. In: *Nature Neuroscience* 22.11 (2019), pp. 1761–1770.
- [34] C. Rudin. “Stop explaining black box machine learning models for high stakes decisions and use interpretable models instead”. In: *Nature Machine Intelligence* 1.5 (2019), pp. 206–215.
- [35] N. Ahmad, M. A. J. van Gerven, and L. Ambrogioni. “GAIT-prop: A biologically plausible learning rule derived from backpropagation of error”. In: *Advances in Neural Information Processing Systems 33* (2020).
- [36] M. Ernault et al. “Equilibrium Propagation with Continual Weight Updates”. In: (Apr. 2020). ArXiv: 2005.04168 (cs.NE).
- [37] T. P. Lillicrap et al. “Backpropagation and the brain”. In: *Nature Reviews Neuroscience* 21.6 (2020), pp. 335–346.
- [38] V. Ranganathan and A. Lewandowski. “ZORB: A derivative-free backpropagation algorithm for neural networks”. In: *ArXiv* (2020). arXiv: 2011.08895 [cs.LG].
- [39] N. Ahmad, L. Ambrogioni, and M. A. J. van Gerven. “Overcoming the weight transport problem via spike-timing-dependent weight inference”. In: *NBDT* 5.3 (2021), pp. 1–20.
- [40] A. Payeur et al. “Burst-dependent synaptic plasticity can coordinate learning in hierarchical circuits”. In: *Nat. Neurosci.* 24.7 (July 2021), pp. 1010–1019.
- [41] S. Wang. “Efficient deep learning”. In: *Nature Computational Science* 1.3 (2021), pp. 181–182.
- [42] Y. LeCun, C. Cortes, and C. J. Burges. *The MNIST database of handwritten digits*. AT&T Labs [Online]. Available: <http://yann.lecun.com/exdb/mnist>.

A COPI Pseudocode

Algorithm 1 demonstrates COPI training of a deep feedforward neural network using a quadratic loss. For illustration, we use backpropagation-based perturbations δ_l^{bp} .

Algorithm 1 Constrained Parameter Inference

```
1: procedure COPI(network, data)
  ▷ network consists of randomly initialized forward weight matrices  $W_l$  and lateral weight
  matrices  $R_l$  with  $1 \leq l \leq L$ 
  ▷ data consists of  $N$  input-output pairs  $(y_0, y^*)$ 
  ▷ Parameters: learning rates  $\eta_R$  and  $\eta_W$ ; number of epochs; batch size
2:   for each epoch do
3:     for each batch =  $\{(y_0, y^*)\} \subset \text{data}$  do
      ▷ Forward pass
4:       for layer  $l$  from 1 to  $L$  do
5:          $x_l = R_l y_{l-1}$                                      ▷ Decorrelate the input data
6:          $a_l = W_l x_l$                                        ▷ Compute activation
7:          $y_l = f(a_l)$                                        ▷ Compute output
8:       end for
9:        $\ell = \|y_L - y^*\|^2$                                      ▷ Compute loss
      ▷ Backward pass
10:      for layer  $l$  from  $L$  to 1 do
11:         $\delta_l = -\frac{d\ell}{da_L}$  if  $l = L$  else  $\delta_l = \frac{da_{l+1}}{da_l} \delta_{l+1}$    ▷ Compute learning signal
12:      end for
      ▷ Update Parameters (mix passes)
13:      for layer  $l$  from  $L$  to 1 do
14:         $W_l \leftarrow W_l + \eta_W ((a_l + \delta_l)x_l^\top - W_l \text{diag}(x_l^2))$    ▷ Update forward weights
15:         $R_l \leftarrow R_l - \eta_R ((R_l x_l) x_l^\top - R_l \text{diag}(x_l^2))$    ▷ Update lateral weights
16:      end for
17:    end for
18:  end for
19:  return network
20: end procedure
```

B Compressing COPI networks

Here we describe how the presence of decorrelated inputs at every network layer enables the compression of a network. Specifically, we make use of these decorrelated inputs in order to approximate multiple (non-linear) layer transformations with a linear matrix.

Consider a system in which one has access to some empirical dataset, $X \in \mathbb{R}^{M \times N}$, where M is the number of features and N the number of datapoints. Suppose also, that there exists some (potentially non-linear) transformation of this dataset, such that $Z = f(X) \in \mathbb{R}^{P \times N}$, where $f(\cdot)$ is some arbitrary function and P is the dimensionality of the transformed data. We could then suppose that we can compute a linear approximation of the function $f(\cdot)$, such that

$$Z \approx WX.$$

Supposing that we take this approximation for granted, we might then attempt to solve for the matrix W by

$$Z = WX \Rightarrow W = ZX^{-1}.$$

This would only be possible if X was invertible and square. Naturally, a pseudo-inverse could also be deployed, though this is expensive to compute. For such an approach to learning in deep networks, see [38].

Alternatively, we could (as carried out within the derivation of COPI) multiply our original formulation by the transpose of our data, such that

$$Z = WX \Rightarrow ZX^\top = WXX^\top \Rightarrow W = ZX^\top (XX^\top)^{-1},$$

where we have now shifted away from an inverse of the data to, instead, the inverse of its correlation matrix. However, we nonetheless still require an (expensive) computation of a matrix inverse. In the case of networks trained to have decorrelated inputs at every layer, we can choose these inputs as our input data, such that $(XX^\top)^{-1} = \text{diag}(1/x_1x_1^\top, \dots, 1/x_Mx_M^\top) \triangleq D$ for these layer activities

with x_m the m th row of X . This allows us to compute a transformation from such decorrelated inputs as

$$W = ZX^\top D.$$

Thus, in networks with decorrelated layer-wise inputs or activities, linear approximations of transformations can be computed without computing inverses. This is ultimately the mechanism by which COPI also operates, though in a sample/batch-wise manner with a changing output distribution (due to the learning signals). Specifically, consider the COPI algorithm at its ‘fixed point’, where $\Delta_{W_i}^{\text{copi}} = 0 = \mathbb{E}[z_l x_l^\top] - W_l \text{diag}(\mathbb{E}[x_l^2])$. Under this condition, we could re-arrange to say that $W_l = \mathbb{E}[z_l x_l^\top] \text{diag}(\mathbb{E}[x_l^2])^{-1}$, equivalent to our above formulation but under the assumption that we have a fixed, desired output, z_l , unlike the case where we wish to compute stochastic errors and do online learning.

The MNIST dataset consists of many input pixels with a consistently zero activation across all data samples (in the periphery). Due to this, the removal of hidden layers was carried out by removal of layers following the first network layer and the first network layer was never removed. This ensured that our decorrelated data, X , used for the determination of a linear approximation, had no elements which were zero and thus we could divide by X without issue.

C Single-weight updates

Let us consider the COPI update for single synaptic weights, given by

$$\begin{aligned}\Delta_{w_{ij}}^{\text{copi}} &= z_i x_j - w_{ij} x_j^2 = \left(\sum_j w_{ij} x_j \right) x_j - w_{ij} x_j^2 + \delta_i x_j \\ \Delta_{r_{ij}}^{\text{copi}} &= -(\tilde{z}_i x_j - r_{ij} x_j^2) = \left(\sum_j (-r_{ij}) x_j \right) x_j - (-r_{ij}) x_j^2.\end{aligned}$$

The first term in both expressions is a Hebbian update which relies on the states of the pre-synaptic units x_j and post-synaptic units z_i or \tilde{z}_i only. The second term in both expressions takes the form of a weight decay. This functional form is similar to Oja’s rule [2], which states:

$$\Delta_{m_{ij}}^{\text{oja}} = y_i x_j - m_{ij} y_i^2 = \left(\sum_j m_{ij} x_j \right) x_j - m_{ij} y_i^2$$

for $y = Mx$. COPI differs from Oja’s rule in that the forward weight update has an additional term $\delta_i x_j$ and the weight decay for both the forward and lateral weights depends on the (squared) pre-synaptic rather than post-synaptic firing rates. The functional impact of the difference in the weight decay scaling (by post- vs pre-synaptic firing rates), is that Oja’s rule scales weight decay in order to normalize the scale of the weights which target a post-synaptic neuron. By comparison, COPI scales the weight decay in order to best infer the scale which the weights should take in order to reproduce the post-synaptic neuron activity given the observed pre-synaptic neuron activity.

D Code, implementation, and compute

All code used to produce the figures present in the results section of the main paper are present in a repository available at: <https://github.com/nasiryahm/ConstrainedParameterInference>.

All simulations were produced using in a Python3 environment (package list available in the code zip) and executed using NVIDIA Quadro RTX 6000 GPUs in a system with an Intel(R) Xeon(R) Gold 5218 CPU (64GB RAM).